Journal of ELECTRONIC MATERIALS, Vol. 49, No. 8, 2020
https://doi.org/10.1007/s11664-020-08246-z

Synthesis of CuO Nanoflowers and Their Application Towards Inflammable Gas Sensing

SHARMI GANGULY ,[1,4] RAVINDRA JHA,[2] PRASANTA K. GUHA,[2,3] and CHACKO JACOB[1,2]

1.—Materials Science Centre, Indian Institute of Technology, Kharagpur, West Bengal 721302, India. 2.—ATDC, Indian Institute of Technology, Kharagpur, West Bengal 721302, India. 3.—Department of Electronics and Electrical Communication Engineering, Indian Institute of Technology, Kharagpur, West Bengal 721302, India. 4.—e-mail: s.gangulyei@gmail.com

Copper oxide (CuO) nanoflowers were synthesized by a reproducible and inexpensive wet chemical method. The synthesized CuO nanoflowers were characterized by x-ray diffraction, Raman spectroscopy, x-ray photoelectron spectroscopy, field emission scanning electron microscopy and energy-dispersive spectroscopy. For an optimized operating temperature of 240°C, the sensor characteristics of the gas sensing device were measured using acetone as a volatile gas. The synthesized CuO nanoflower-based gas sensor responded very strongly for acetone gas concentrations in the range of 250–2250 ppm, and the recorded response for concentrations of 250 ppm and 2250 ppm was 2.7 and 7.2, respectively. The stability of the synthesized sensor was checked by repeating the measurements over a period of 1 month, and a very small change of 3.3% in the response of the sensor was observed.

Key words: Wet chemical, nanoflower, gas sensor, VOCs, sensitivity

INTRODUCTION

Over the past few years, the increase in the number of industries producing toxic gases and flammable volatile organic compounds (VOCs) has resulted in alarming levels of environmental pollution, with serious impacts on human safety.[1,2] The detection of these VOCs and other toxic gases has attracted considerable attention within the scientific community. Various public agencies, including the National Institute of Occupational Safety and Health (NIOSH, USA) and the Occupational Safety and Health Administration (OSHA, USA), have established recommended exposure limits for specific VOCs.[3] Acetone is a potentially hazardous, volatile and inflammable chemical solvent that is used in both industry and research laboratories on a large scale.[4] Thus, from the perspective of human safety and health, the detection of acetone in the workplace is critical. Moreover, detection of acetone is a salient feature in diagnosing human diseases[5,6] and as reference data to determine the quality of food.[7]

Semiconducting nanomaterials, which have a large surface-area-to-volume ratio, are promising candidates for gas sensing applications. Semiconductor metal oxides attract special attention due to their good electrical and optical properties, high sensitivity and low manufacturing cost.[8–11] Gas sensors made of *n*-type semiconductors have been commercialized; however, *p*-type semiconductor-based gas sensors exhibit a better response.[12] For an *n*-type gas sensor based on semiconducting oxides, electrons are depleted from the semiconductor, whereas for *p*-type sensors, holes accumulate when negatively charged oxygen is absorbed.[13] Thus, upon exposure of these materials to VOCs, there is a reduction in the bulk resistance of *n*-type metal oxide semiconductors, whereas there is an increase in resistance for *p*-type metal oxide gas sensors. Various types of gas sensors have been

(Received January 7, 2020; accepted May 28, 2020; published online June 13, 2020)

reported in the literature, including optical, field effect, acoustic wave, organic and oxide-based semiconductor sensors.[14–18] In 2012, Liu et al. surveyed gas sensors, focusing on sensitivity and selectivity as performance indicators to compare different sensing technologies.[19] Steinhauer et al.[20,21] synthesized several types of CuO nanowire sensors by thermal oxidation and studied their response to H_2S gas at the ppb level. A device was developed by Zhang et al.[22] where leaflet-like CuO nanosheets were synthesized by a solution method, and its sensing properties towards H_2S gas was investigated. CuO nanowires used for NO_2 gas sensing in automotive cabin applications were proposed by Lee et al.[23] at a temperature of 300°C for an NO_2concentration of 30–100 ppm. Mashock et al.[24] reported that CuO nanowires combined with SnO_2nanocrystals were able to sense 1% NH_3 in the air. Aslani and co-workers synthesized CuO nanoparticles by a solvothermal wet chemical route, which responded to CO gas at a temperature of 300°C.[25] In 2011, Parmar et al. synthesized CuO thin films for sensing two important VOCs, methanol and ethanol, at 350°C and 400°C, respectively.[26] CuO flower-like gas sensing devices were recently synthesized by Liu and his group, with good response and recovery time for sensing of formaldehyde.[27] In the past few years, semiconductor metal oxides such as InN and SnO_2 have been fabricated for the detection of acetone gas at elevated temperatures.[28–30] In most investigations, the sensing behavior of acetone and ethanol is similar, due to their analogous chemical characteristics.[30,31] Therefore, the fabrication of a gas sensor which can distinguish between acetone and ethanol is a significant challenge. Moreover, in practical applications, devices with high sensitivity, selectivity and stability (the so-called 3 S's of a gas sensor) are desirable for developing an efficient gas sensor.[32]

In this study, single-crystal CuO nanoflowers were synthesized by an inexpensive and rapid wet chemical method. The gas sensor device was fabricated by depositing nickel contacts on the synthesized CuO nanostructures, and the gas sensing behavior of these CuO nanoflowers was studied using acetone, ethanol, methanol, isopropyl alcohol, toluene and chloroform and ammonia gas at relatively low temperature. Repeatability studies were performed with acetone on the CuO sensor device.

MATERIALS AND METHOD

Synthesis of CuO Nanoflowers

Copper foil (99.99% purity, Sigma Aldrich) was successively cleaned with dilute nitric acid (0.5 wt.%), ethanol and deionized water and cut into small pieces to be used as the source for e-beam evaporation. The glass slides were also cleaned in ethanol and deionized water and dried at 75°C. A thin film of Cu was deposited on the glass slide by electron beam (e-beam) evaporation. The glass slides with Cu deposited on them were then carefully dipped in 50 ml sodium hydroxide (NaOH) (3 M) and 50 ml ammonium persulphate ($(NH_4)_2S_2O_8$) (0.15 M) for 12 h to form CuO on the glass slide. The glass slides with CuO were then cleaned with deionized water and ethanol and dried. A uniform black film of CuO nanoflowers on the glass slides was confirmed by different characterization techniques. The samples were then further processed for fabricating gas sensing devices.

Fabrication of the Gas Sensing Device

Electrical contacts were made with nickel on the fabricated CuO nanoflower slides by evaporation using an appropriate mask. For making electrical contacts, nickel was used, since the work function of nickel is reported to be 5.01 eV, and the work function of copper oxide is reported as 5.2–5.6 eV. The complete gas sensing device is schematically represented in Fig. 1.

Gas Sensing Instrument

The sensing properties of the CuO sensor were measured using a Precision Semiconductor Parameter Analyzer (Agilent 4156C). A block diagram of the system used to test the gas sensor is shown in supplementary Figure S1.

In such systems, the response is defined by the following equation

$$\text{Response} = R_{\text{gas}} - R_{\text{air}}/R_{\text{air}} \quad (1)$$

where R_{gas} denotes the sensor resistance in the presence of the target gas, and R_{air} defines the sensor resistance in dry air. The response time t_{res} and recovery time t_{rec} are defined as the time required for the sensors to achieve 90% of the total resistance change in the case of adsorption and desorption, respectively.

RESULTS AND DISCUSSION

Characterization of the CuO Nanoflowers

The x-ray diffraction (XRD) data confirmed the formation of the CuO phase. The diffractogram of the copper film after chemical treatment for 12 h is shown in Fig. 2a. The sample was scanned over a

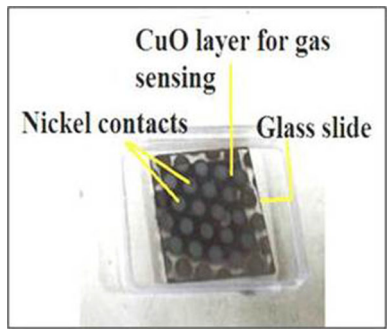

Fig. 1. Device for gas sensing application.

range from 20° to 80° in increments of 0.05°. The XRD pattern matched the Joint Committee on Powder Diffraction Standards (JCPDS) Card No. 48-1548, from which it was concluded that the two peaks of CuO appearing at 35.52° and 38.70° correspond to the $(11\bar{1})$ and (111) planes, respectively. Other weaker peaks of CuO which appeared at 48.72° and 61.94° correspond to the $(20\bar{2})$ and $(11\bar{3})$ planes, respectively. Thus, the obtained sample was crystalline with a monoclinic structure. The broad peak below 30° is from the glass substrate. CuO belongs to the C2/c space group with two molecules per primitive cell. The zone center optical phonon modes with symmetries are $\Gamma = 4A_u + 5B_u + A_g + 2B_g$. Only three $A_g + 2B_g$ modes are Raman-active.[33,34] Three major peaks are observed at 291 cm^{-1}, 337 cm^{-1} and 619 cm^{-1} in the Raman spectrum of the CuO sample (Fig. 2b). The peak at 291 cm^{-1}corresponds to the A_g mode, and the peaks at 337 and 619 cm^{-1} correspond to the B_g modes. The fourth broadened peak at 1088 cm^{-1} is due to the presence of a multi-phonon transition. The major peaks of the Raman spectrum were shifted slightly to larger wave numbers compared with bulk CuO nanostructures, and this was in good agreement with literature values.[35] The absence of Cu_2O modes in the Raman spectrum confirmed the phase purity of the CuO on the glass slides, which was also supported by the XRD pattern. Figure 2c shows the x-ray photoelectron spectroscopy (XPS) spectrum of the CuO nanostructures, where the Cu $2p_{3/2}$ and Cu $2p_{1/2}$ major peaks are centered at 933.30 eV and 953.32 eV, respectively.

The binding energy gap calculated between the Cu $2p_{3/2}$ and Cu $2p_{1/2}$ peaks was 19.98 eV, which agreed with the literature values.[36] The shake-up satellite peaks of the Cu $2p_{3/2}$ and Cu $2p_{1/2}$ at 942.4 eV and 962.6 eV, respectively (9 eV greater than the corresponding major peaks), confirmed the formation of Cu^{2+} on the surface of the glass slides.[37,38] According to the literature, the position of the Cu $2p_{3/2}$ peak for CuO appears at a binding energy of 933.5 eV. The oxygen O 1s peaks were fitted into three components using a Gaussian function, and this is shown in Fig. 2d. The peaks were centered at 529.48 eV, 531.03 eV and 532.05 eV, corresponding to oxygen binding in the lattice of CuO, –OH groups and H_2O, respectively.[39,40] The XPS spectrum confirmed that the synthesized film on the glass slides was composed of pure stoichiometric CuO phase.

The surface morphologies of the CuO films grown on glass slides were investigated by field emission

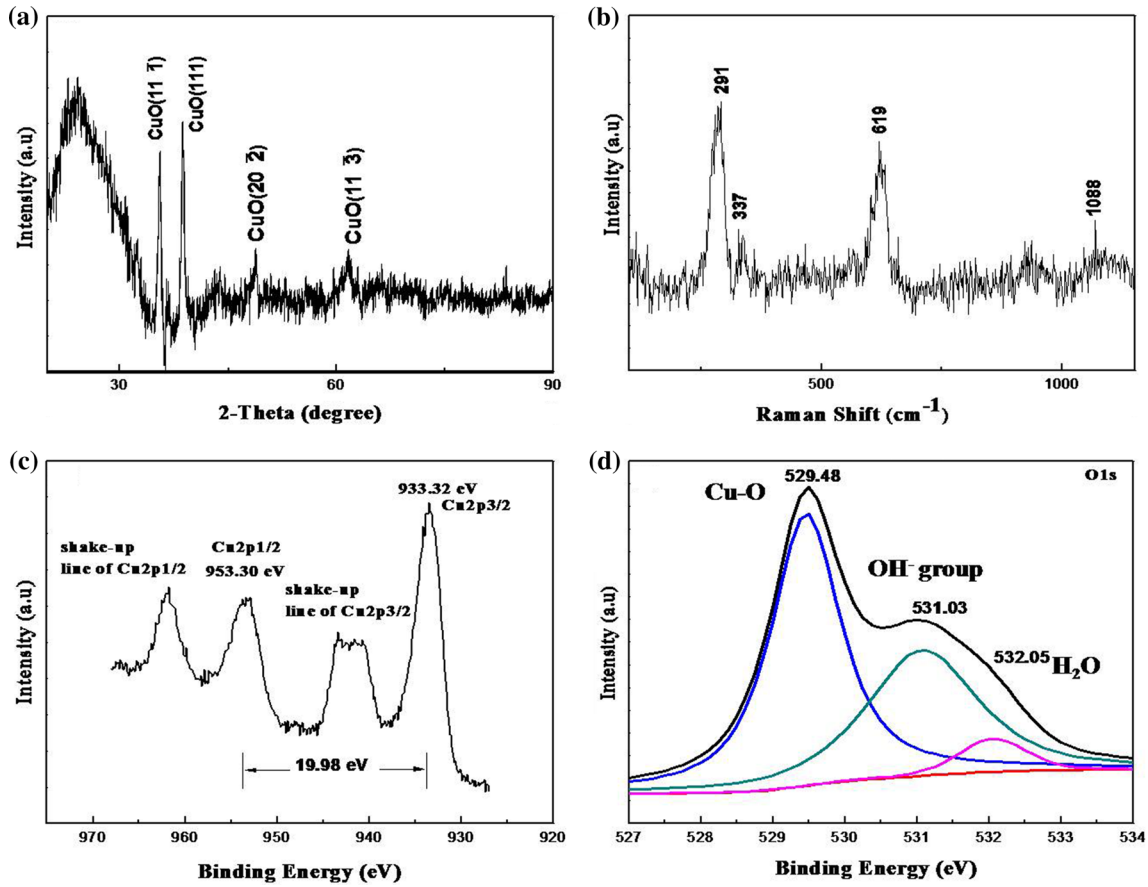

Fig. 2. (a) XRD pattern of CuO on a glass slide, (b) Raman spectrum of the copper oxide nanostructures, (c) XPS spectra of the copper oxide nanostructures showing the Cu 2*p* region and (d) the deconvoluted O 1s peak.

scanning electron microscopy (FESEM) and are shown in Fig. 3. Flower-like structures of CuO were observed (Fig. 3a) on the glass slides. On magnification (Fig. 3a), it was observed that smaller flakes were rearranged to form flower-like structures all over the place (Fig. 3b, c and d).

The energy-dispersive spectroscopy (EDS) spectrum of the synthesized sample is shown in supplementary Figure S2. The internal structure of the CuO nanoflowers was analyzed by transmission electron microscopy (TEM). The TEM images (Fig. 4a and b) show the CuO flakes. In addition, a selected area electron diffraction (SAED) pattern (Fig. 4c) was taken from a particular region of a flake, as shown in Fig. 4b. The interplanar spacing was calculated from the lattice fringe pattern (Fig. 4d) and found to be $d = 0.229$ nm, which corresponds to the (111) plane of CuO.

Gas Sensing Behavior of CuO Nanoflowers

In general, a gas sensor device's response varies with temperature, and a change in the operating temperature of a semiconductor metal oxide sensor leads to a resistance change in the sensor. The gas sensor chamber was heated for an hour before the sensor properties were measured. The gas sensing response of the CuO nanoflowers was tested using different VOCs (acetone, ethanol, methanol, IPA, toluene and chloroform) and NH_3. All the gases were tested at an intermediate concentration of 1250 ppm in the gas sensing instrument shown in Fig. 5a. The CuO nanoflower gas sensing device showed a good response to acetone vapor in all the tested gases. Thus, the sensor was further tested with acetone by exposing it to acetone at a concentration of 1250 ppm at various temperatures from 50°C to 420°C, and the results are shown in Fig. 5b. It can be observed from Fig. 5b that as the temperature of the gas chamber increased, the sensing response of the CuO device for acetone vapor decreased. With increasing temperature, the oxygen concentration in the gas chamber decreased, which resulted in a gradual decrease in the gas sensing efficiency of CuO beyond a certain temperature. The maximum gas sensing response of CuO was observed at a temperature of 240°C. This optimum operating temperature is significantly lower than the values reported in the literature for acetone sensing using CuO, which are usually above 300°C.[26,43–45] The response ($R_{gas} - R_{air}/R_{air}$) of the CuO nanoflower gas sensor to acetone vapor at concentrations of 250 ppm and 2250 ppm was 2.7 and 7.2, respectively, as shown in Fig. 5c. These values are slightly higher than the reported values.[26,44,45] The on and off times of the experiment were 900 s each. Response and recovery times of 490 s and 240 s, respectively, were observed at an acetone concentration 1250 ppm. The gas sensor's response with varying concentrations of acetone is also represented in Fig. 5c. The CuO gas sensor showed a response of approximately 2.7 at an acetone concentration of 250 ppm, which indicated good sensing properties of the device for acetone vapor.

The sensitivity of the sensor can be empirically denoted by the following equation:

$$S = \beta C^n \tag{2}$$

where S denotes response, C is concentration, and the sensitivity is characterized by the pre-factor β

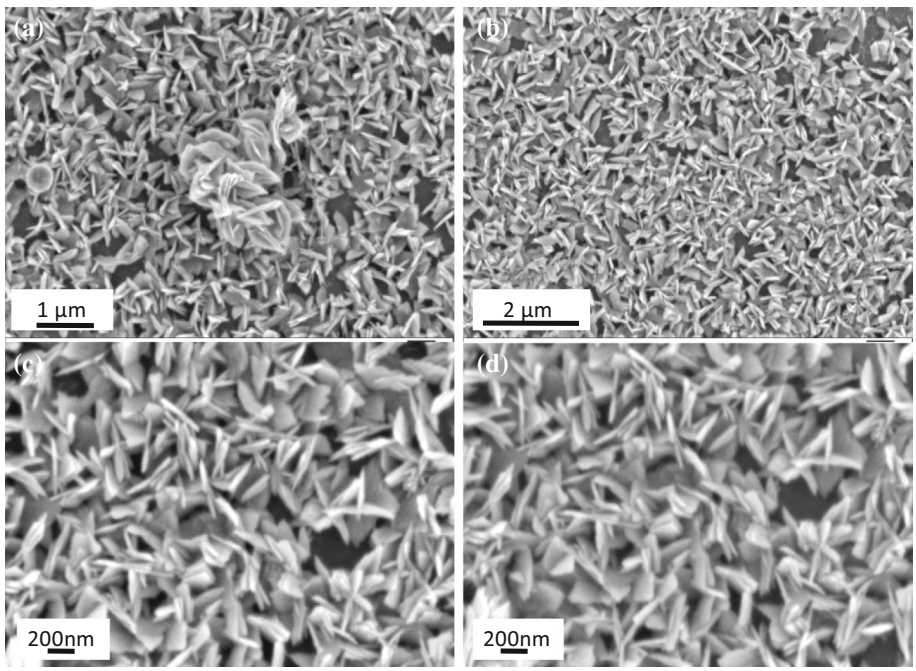

Fig. 3. FESEM images of (a) CuO on a glass slide; (b), (c) and (d) are magnified images of the region shown in "a".

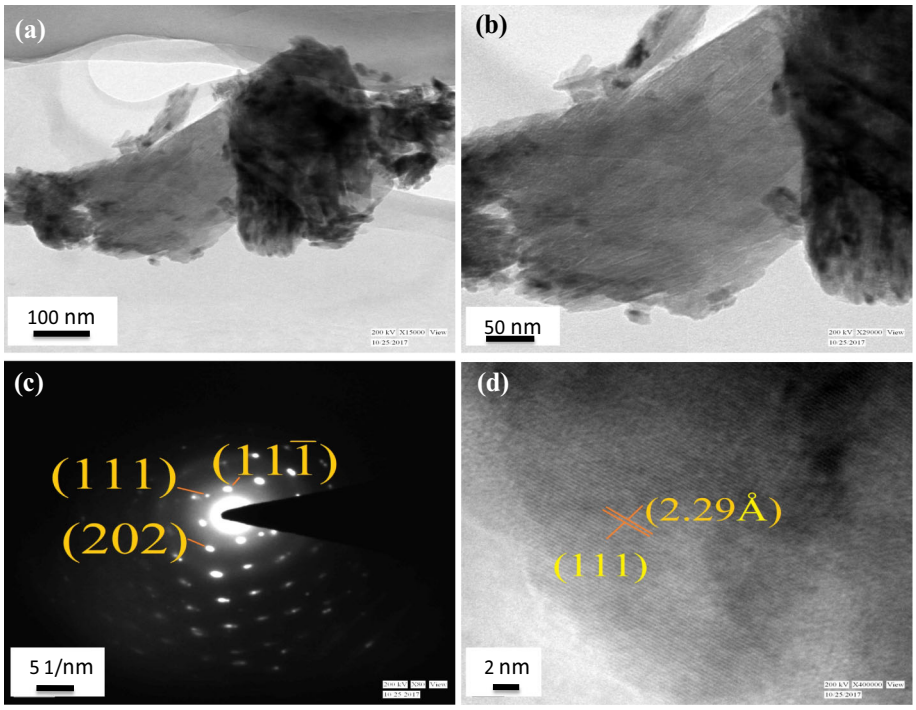

Fig. 4. (a) TEM micrograph of synthesized CuO on a glass slide, (b) magnified portion of image (a). (c) SAED pattern of CuO and (d) lattice fringe of CuO.

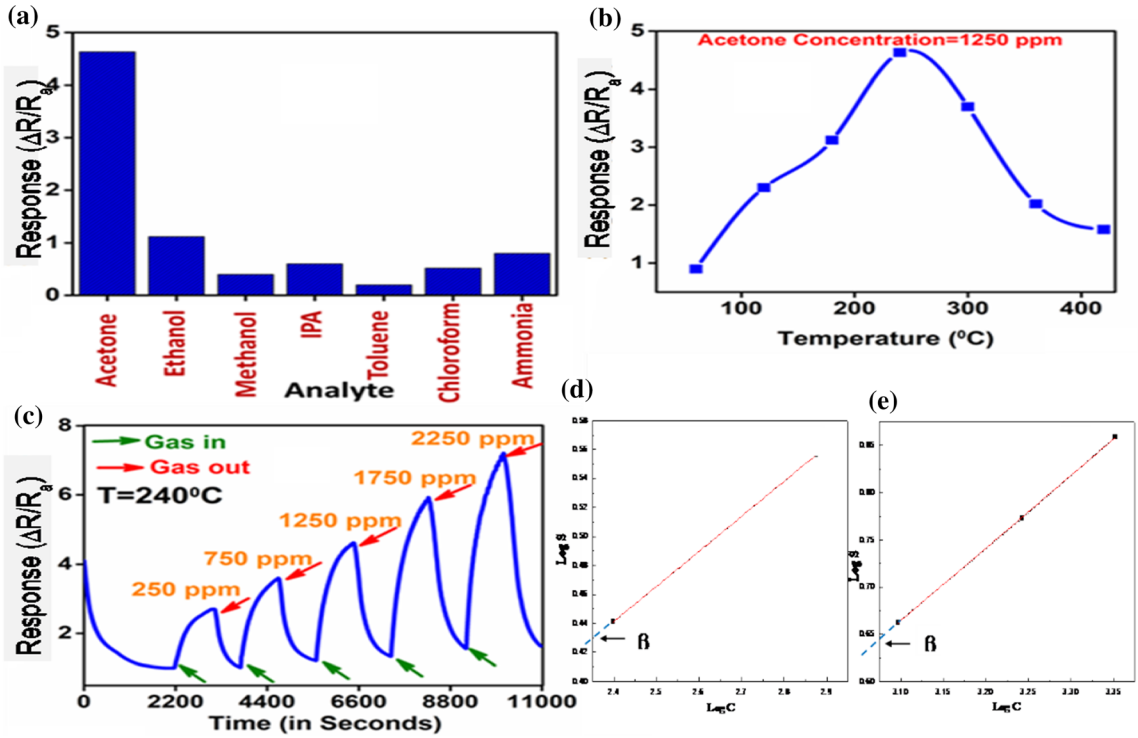

Fig. 5. CuO nanoflower gas sensor device was tested on (a) different VOCs and NH_3, (b) acetone vapor at a fixed concentration (1250 ppm) with varying temperature from 50°C to 420°C, (c) acetone vapor with varying concentrations from 250 ppm to 2250 ppm at 240°C, and (d) sensitivity calculation for lower concentration of acetone vapor and (e) sensitivity calculation for higher concentration of acetone vapor.

and exponent n. n may have some rational fraction value, depending on the charge of the surface species and the stoichiometry of the elementary reactions on the surface. The equation represents how the sensor response would change with small changes in gas concentration. The value of n may be

1 (indicating a linear response) or some other value indicating a non-linear response. If n is 1, then β represents the slope of sensitivity versus concentration curve.

Using Eq. 2 and taking the logarithm on both sides, the figures below were plotted as Log S vs. Log C, which follows the equation of the straight line [$y = mx + c$]. The sensitivity (n) was determined from the slope of the straight line, and Log β, which is a constant, was obtained from the intercept of the straight line. From Fig. 5d and e, the sensitivity was determined to be 0.24 and 0.77 for lower and higher concentrations of acetone gas, respectively.

The response and stability of the synthesized CuO gas sensor were investigated for a period of 1 month, and sensing measurements were performed at 1-week intervals at a fixed concentration of acetone (1250 ppm), as shown in Fig. 6. The change in response was calculated to be 3.3% for the CuO gas sensor over the 1-month period, which indicated the stability and accuracy of the device.

Gas Sensing Mechanism of CuO on Acetone

In the presence of air, oxygen is an electronegative atom which adsorbs onto a surface by taking electrons from p-type material and ionizes to species such as O_2^-, O^- and O^{2-} in the temperature range 100–500°C.[41,42] In the temperature range between 150°C and 400°C, O_2^- is converted into $2O^-$ by the following reactions:[42]

$$O_{2\,gas} + e^- \leftrightarrow O^-_{2\,ads} \quad (3)$$

$$O^-_{2\,ads} + e^- \leftrightarrow 2O^-_{ads} \quad (4)$$

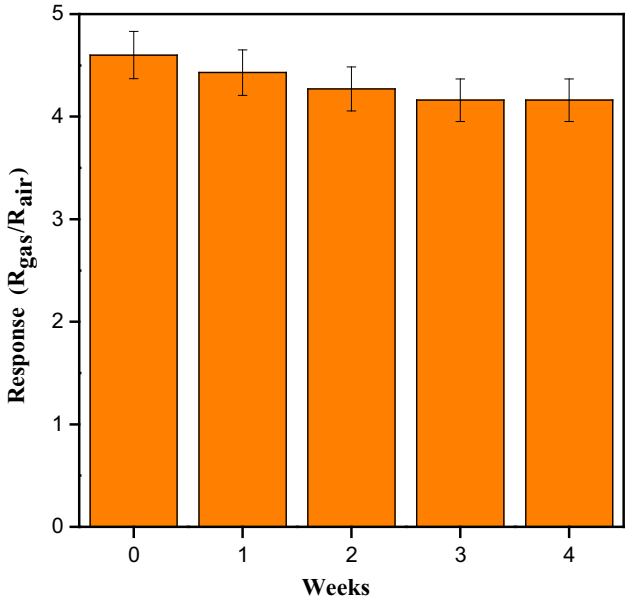

Fig. 6. The response of the CuO gas sensor to acetone vapor (1250 ppm) for a period of 1 month.

$$O^-_{ads} + e^- \leftrightarrow O^{2-}_{ads} \quad (5)$$

where the subscripts 'gas' and 'ads' denote gaseous and adsorbed oxygen, respectively. CuO is a p-type material and has more holes than electrons. When the CuO gas sensor is heated to 240°C in the presence of air, oxygen from the air is adsorbed onto the CuO device and creates more holes close to the surface, resulting in a hole accumulation layer on the surface. At this temperature, when the reducing gas is introduced into the gas chamber, the reducing gas is oxidized by the adsorbed surface $2O^-$ and releases electrons onto the surface of the device, which in turn increases the sensor resistance, as shown in Fig. 7. For instance, the CuO gas sensing device sensed acetone vapor more strongly with respect to other VOCs due to the availability of electrons in acetone vapor. The electron-donating inductive effect of two methyl groups increased the electron density in the oxygen atom of acetone vapor, which was readily available for donating to the CuO. The thin film of CuO nanoflowers on the glass slides has a large surface-area-to-volume ratio, resulting in increased contact between the copper oxide and vapor, and this could be a contributing factor for the enhanced gas sensing performance.

CONCLUSIONS

A CuO nanoflower gas sensing device was successfully fabricated using a rapid and inexpensive method and showed a stable sensing response. The response of the p-type device was tested on various VOCs at a fixed temperature. The response of the gas sensing device without any additives or dopant was shown to be good for acetone vapor over a period of 1 month. The sensing temperature was comparatively low (240°C) with respect to other metal oxides and values reported in the literature, where the operating temperatures were above 300°C.[26,43–45] The highest response calculated for an acetone concentration of 2250 ppm was 7.2, which was also more than the reported values.[26,44,45] In the literature, sensing of acetone gas at concentrations below 250 ppm has been demonstrated, and there is no reason to believe (other than our present experimental limitations) that such lower values cannot be sensed by our sensor. The

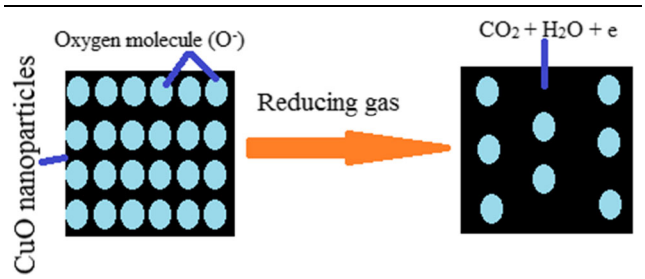

Fig. 7. A schematic of the gas sensing mechanism of the CuO nanoparticles in the presence of air and reducing gases.

"3 S" properties (sensitivity, selectivity and stability) of this device could make it a promising alternative for the detection of acetone in the human body and everyday life, as well as in industry.

ACKNOWLEDGMENTS

This work was supported by IIT Kharagpur, India. The XRD and SEM characterization was performed at CRF (Central Research Facility), IIT Kharagpur. XPS was measured in the DST FIST Facility of the Physics Department, IIT Kharagpur.

ELECTRONIC SUPPLEMENTARY MATERIAL

The online version of this article (https://doi.org/10.1007/s11664-020-08246-z) contains supplementary material, which is available to authorized users.

REFERENCES

1. X. Chen, C.K.Y. Wong, C.A. Yuan, and G. Zhang, *Sens. Actuators, B* 177, 178 (2013).
2. E. Kanazawa, G. Sakai, K. Shimanoe, Y. Kanmura, Y. Teraoka, N. Miura, and N. Yamazoe, *Sens. Actuators, B* 77, 72 (2001).
3. G. Eranna, *Metal Oxide Nanostructures as Gas Sensing Devices* (Boca Raton: CRC Press, 2011), p. 291.
4. X. Liu, J. Hu, B. Cheng, H. Qin, and M. Jiang, *Sens. Actuators, B* 134, 483 (2008).
5. N. Makisimovich, V. Vorotyntsev, N. Nikitina, O. Kaskevich, P. Karabun, and F. Martynenko, *Sens. Actuators, B* 36, 419 (1996).
6. S.S. Likhodii, K. Musa, and S.C. Cunnane, *Clin. Chem.* 48, 115 (2002).
7. A.M. Taurino, C. Distante, P. Siciliano, and L. Vasanelli, *Sens. Actuators, B* 93, 117 (2003).
8. R.L. Vander Waal, G.W. Hunter, J.C. Xu, M.J. Kulis, G.M. Berger, and T.M. Ticich, *Sens. Actuators, B* 138, 113 (2009).
9. N. Barsan, D. Koziej, and U. Weimar, *Sens. Actuators, B* 121, 18 (2007).
10. Y. Zhang, T. Liu, L. Lin, S. Hussain, S. Wu, W. Zeng, S. Cao, F. Pan, and X. Peng, *J. Mater. Sci.: Mater. Electron.* 25, 376 (2014).
11. Y. Zhang, J. Hu, B.A. Bernevig, X. Wang, X. Xie, and W. Liu, *Phys. Rev. Lett.* 102, 106401 (2009).
12. M. Hübner, C.E. Simion, A. Tomescu-Stănoiu, S. Pokhrel, N. Bârsan, and U. Weimar, *Sens. Actuators, B* 153, 347 (2011).
13. F. Wang, H. Li, Z. Yuan, Y. Sun, F. Chang, H. Deng, L. Xie, and H. Li, *RSC Adv.* 6, 79343 (2016).
14. M. Ando, T. Kobayashi, S. Iijima, and M. Haruta, *Sens. Actuators, B* 96, 589 (2003).
15. F. Liao, C. Chen, and V. Subramanian, *Sens. Actuators, B* 107, 849 (2005).
16. J.J. Miasik, A. Hooper, and B.C. Tofield, *J. Chem. Soc. Faraday Trans. 1* 82, 1117 (1986).
17. N. Peng, Q. Zhang, Y.C. Lee, O.K. Tan, and N. Marzari, *Sens. Actuators, B* 132, 191 (2008).
18. M. Penza, P. Aversa, G. Cassano, W. Wlodarski, and K. Kalantarzadeh, *Sens. Actuators, B* 127, 168 (2007).
19. X. Liu, S. Cheng, H. Liu, S. Hu, D. Zhang, and H. Ning, *Sensors* 12, 9635 (2012).
20. S. Steinhauer, E. Brunet, T. Maier, G.C. Mutinati, and A. Kock, *Sens. Actuators, B* 186, 550 (2013).
21. S. Steinhauer, E. Brunet, T. Maier, G.C. Mutinati, A. Kock, O. Freudenberg, C. Gspan, W. Grogger, A. Neuhold, and R. Resel, *Sens. Actuators, B* 187, 50 (2013).
22. F. Zhang, A. Zhu, Y. Luo, Y. Tian, J. Yang, and Y. Qin, *J. Phys. Chem. C* 114, 19214 (2010).
23. Y.S. Kim, I.S. Hwang, S.J. Kim, C.Y. Lee, and H. Lee, *Sens. Actuators, B* 135, 298 (2008).
24. M. Mashock, K.H. Yu, S.M. Cui, S. Mao, G.H. Lu, and J.H. Chen, *ACS Appl. Mater. Interfaces.* 4, 4192 (2012).
25. A. Aslani and V. Oroojpour, *Phys. B* 406, 144 (2011).
26. M. Parmar and K. Rajanna, *Int. J. Smart Sens. Intell. Syst.* 4, 710 (2011).
27. H. Deng, H.R. Li, F. Wang, C.X. Yuan, S. Liu, P. Wang, L.Z. Xie, Y.Z. Sun, and F.Z. Chang, *J. Mater. Sci.: Mater. Electron.* 27, 6766 (2016).
28. K.W. Kao, M.C. Hsu, Y.H. Chang, S. Gwo, and J.A. Yeh, *Sensors* 12, 7157 (2012).
29. L. Qin, J. Xu, X. Dong, Q. Pan, Z. Cheng, Q. Xiang, and F. Li, *Nanotechnology* 19, 185705 (2008).
30. J. Zhao, L.H. Huo, S. Gao, H. Zhao, and J.G. Zhao, *Sens. Actuators, B* 115, 460 (2006).
31. Z. Jing and S. Wu, *Mater. Lett.* 60, 952 (2006).
32. E. Comini, L. Ottini, G. Faglia, and G. Sberveglieri, *IEEE Sens. J.* 4, 17 (2004).
33. J.F. Xu, W. Ji, Z.X. Shen, W.S. Li, S.H. Tang, X.R. Ye, D.Z. Jia, and X.Q. Xin, *J. Raman Spectrosc.* 30, 413 (1999).
34. J. Chrzanowski and J. Irwin, *Solid State Commun.* 70, 11 (1989).
35. V. Cretu, V. Postica, A.K. Mishra, M. Hoppe, I. Tiginyanu, Y.K. Mishra, L. Chow, N.H. de Leeuw, R. Adelung, and O. Lupan, *J. Mater. Chem. A* 4, 6527 (2016).
36. J.S. Shaikh, R.C. Pawar, R.S. Devan, Y.R. Ma, P.P. Salvi, S.S. Kolekar, and P.S. Patil, *Electrochim. Acta* 56, 2127 (2011).
37. J.F. Moulder, W.F. Stickle, P.E. Sobol, and K.D. Bomben, *Handbook of X-Ray Photoelectron Spectroscopy* (Eden Prairie: Perkin Elmer Corporation, 1992).
38. C.C. Chusuei, M.A. Brookshier, and D.W. Goodman, *Langmuir* 15, 2806 (1999).
39. O. Akhavan, *J. Phys. D Appl. Phys.* 41, 235407 (2008).
40. A. Katerski, A. Mere, V. Kazlauskiene, J. Miskinis, A. Saar, L. Matisen, A. Kikas, and M. Krunks, *Thin Solid Films* 516, 7110 (2008).
41. C.O. Park and S. Akbar, *J. Mater. Sci.* 38, 4611 (2003).
42. N. Barsan and U. Weimar, *J. Electroceram.* 7, 143 (2001).
43. H. Yan, X. Tian, J. Sun, and F. Ma, *J. Mater. Sci.: Mater. Electron.* 26, 280 (2015).
44. S.K. Shinde, D.-Y. Kim, G.S. Ghodake, N.C. Maile, A.A. Kadam, D.S. Lee, M.C. Rath, and V.J. Fulari, *Ultrason. Sonochem.* 40, 314 (2018).
45. A. Umar, A.A. Alshahrani, H. Algarni, and R. Kumar, *Sens. Actuators B Chem.* 250, 24 (2017).